

# Specific Heat Capacity at Constant Volume for R125 and R410A at Temperatures from (300 to 400) K and Pressures to 20 MPa

Richard A. Perkins\* and Joseph W. Magee

Physical and Chemical Properties Division, Chemical Science and Technology Laboratory, National Institute of Standards and Technology, Boulder, Colorado 80305-3328

Specific heat capacities at constant volume ( $C_V$ ) were measured with an adiabatic calorimeter for pure pentafluoroethane (R125) and an azeotrope-like mixture of R32 and R125 (R410A) with a mole fraction composition of 0.6975 difluoromethane + 0.3025 pentafluoroethane. Temperatures ranged from 300 K to 400 K, and pressures ranged from 3 MPa to 20 MPa. Measurements were conducted on single-phase liquid and compressed gaseous samples along isochores. Density was reported during each calorimetric experiment. The R410A mixture was gravimetrically prepared from high-purity substances. The principal sources of uncertainty are the temperature-rise measurement and the change-of-volume work adjustment. The expanded relative uncertainty (with a coverage factor  $k = 2$  and thus a 2 SD estimate) for  $C_V$  is estimated to be 2 % for liquid-phase results, increasing to 4 % for gas results (below critical density). The expanded relative uncertainty for density is 0.2 %.

## Introduction

Thermodynamic properties of a fluid may be calculated from knowledge of its ideal gas properties and an accurate equation of state. However, heat capacities derived in this manner often lack sufficient accuracy, since the calculation involves integration of the isochoric curvature  $(\partial^2 P / \partial T^2)_\rho$  as in

$$C_V - C_V^0 = -T \int_0^\rho \left( \frac{\partial^2 P}{\partial T^2} \right)_\rho \frac{d\rho}{\rho^2} \quad (1)$$

where  $C_V^0$  is the ideal gas heat capacity (limit of zero density vapor). The quantity  $(\partial^2 P / \partial T^2)_\rho$  has a small absolute value except in the vicinity of the critical point and is very difficult to measure accurately. For compressed liquid states, additional data are required to apply eq 1 because of the discontinuity of  $(\partial P / \partial T)_\rho$  at the saturation boundary that must be traversed along the path from the low-density ideal gas vapor to the liquid density of interest. This requires knowledge of the vapor pressure and enthalpy of vaporization. Alternatively, the heat capacity of the saturated liquid can be substituted for the ideal gas heat capacity (saturated liquid reference) in eq 1, with integration over the path from the saturated liquid density (rather than zero density) to the compressed liquid density of interest. Direct measurements of heat capacities provide useful checks on calculated heat capacities, when they are available along a path traversing the temperature range of interest.

Knowledge of the thermophysical properties in the critical region is necessary to optimize heat pumps based on mixtures containing R125, since operating temperatures within the cycle can closely approach the critical point. The present measurements fill a data gap in the critical and supercritical regions for pure pentafluoroethane (R125) and mixtures containing difluoromethane (R32) with R125. Isochoric specific heat data have been reported by Lüddecke

and Magee<sup>1</sup> for R125 in the liquid phase from its triple point to 345 K at pressures to 35 MPa. This corresponds to a range of liquid densities from 1.26 g·cm<sup>-3</sup> to 1.62 g·cm<sup>-3</sup>, significantly higher than the critical density of 0.57358 g·cm<sup>-3</sup> for R125. Magee<sup>2</sup> reported isochoric specific heat measurements for a mixture of 0.4996 mole fraction R32 + 0.5004 mole fraction R125.

Heat capacities are reported at temperatures from near ambient to 400 K for pure R125 and for an azeotrope-like mixture (R410A) composed of 0.6975 R32 + 0.3025 R125. In addition, densities calculated from the sample mass measurements and the calibrated volume of the calorimeter bomb are reported. The present data cover the range from less than the critical density to over twice the critical density for both the R125 and the R410A mixture.

## Experimental Section

**Materials.** High-purity samples (electronic grade) of R125 and R32 were used to gravimetrically prepare the R410A mixture (nominally 0.5 R125 + 0.5 R32 by mass). The R125 sample that was measured and also used for the R410A mixture had a mole fraction purity of at least 0.9999. The R32 sample used for the R410A mixture also had a mole fraction purity of at least 0.9999. The water content of both pure samples was less than 5 ppm by volume. The R410A mixture components were weighed into a cleaned and evacuated aluminum sample cylinder with a volume of 15 L. The mass fraction of the gas sample in the R410A mixture was 0.500134 R125 + 0.499866 R32 (assuming pure components). This corresponds to a mole fraction composition of 0.6975 R32 + 0.3025 R125 based on the purity of the R32 and R125 samples. The final pressure of the mixture in the sample cylinder was significantly less than the dew-point pressure at ambient temperature, to ensure that the sample remained single phase and the composition did not change when sample was withdrawn to charge the measurement apparatus.

**Measurements.** A twin-bomb adiabatic calorimeter was used for these measurements. Since this apparatus has

\* Corresponding author. E-mail: richard.perkins@nist.gov.

been described in detail by Magee et al.,<sup>3</sup> only a brief discussion will be given here. A spherical bomb contains a sample of well-established mass. A second nearly identical bomb serves as a reference. The volume of the bomb, approximately 70 cm<sup>3</sup>, is a function of temperature and pressure. A platinum resistance thermometer is attached to the sample bombs for the temperature measurement. Temperatures are reported on the ITS-90, after conversions from the original calibration on the IPTS-68 are made. Pressures are measured with an oscillating quartz crystal pressure transducer with a (0 to 20) MPa range. Adiabatic conditions are ensured by a high vacuum (3 × 10<sup>-3</sup> Pa) in the vacuum space surrounding each calorimeter, by a temperature-controlled radiation shield and by a temperature-controlled guard ring, which thermally anchors the filling capillary and the lead wires to the bomb temperature.

For the isochoric heat capacity measurement, a precisely determined electrical energy ( $Q$ ) was applied, and the resulting temperature rise ( $\Delta T = T_2 - T_1$ ) was measured. We obtained the heat capacity from

$$C_V = \left( \frac{\partial U}{\partial T} \right)_V \cong \frac{\Delta Q - \Delta Q_0 - W_{PV}}{m \Delta T} \quad (2)$$

where  $U$  is the internal energy,  $\Delta Q_0 = Q_{0,\text{sam}} - Q_{0,\text{ref}}$  is the energy difference between the sample and reference cells when both bombs are empty,  $\Delta Q = Q_{\text{sam}} - Q_{\text{ref}}$  refers to the energy added during an experiment with a sample,  $W_{PV}$  is the change-of-volume work due to the slight dilation of the bomb, and  $m$  is the mass of substance enclosed in the sample bomb. In this work, the bomb was charged with sample up to the ( $P$ ,  $T$ ) conditions of the highest density isochore to be measured. The bomb and its contents were cooled to a starting temperature in the single-phase liquid region. Measurements were then performed in that region with increasing temperatures until either the upper temperature (400 K) or the upper pressure limit (20 MPa) was attained. At the completion of a run, a small part of the sample was cryopumped into a lightweight cylinder. The next run was started with a lower density. When the runs were completed, the remaining sample was discharged and weighed. A series of such runs from different fillings completes the investigation of the ( $P$ ,  $T$ ,  $C_V$ ) surface. Each mass increment was determined from the difference of weighings of the lightweight cylinder made with a sensitive (10<sup>-4</sup> g) balance. Small adjustments were made to each mass increment for changes in air buoyancy. The mass of the sample was determined from the sum of the appropriate mass increments for each isochore.

**Assessment of Uncertainties.** Uncertainty in the  $C_V$  determination has been discussed in detail.<sup>3</sup> The accuracy of this method is limited by the uncertainty involved in the measurement of temperature rise and the change-of-volume work adjustment. We use a definition for the expanded uncertainty that is two times the standard uncertainty (i.e., a coverage factor  $k = 2$  and thus a 2 standard deviation (SD) estimate). For the mixture, there is slightly increased uncertainty in specific heat of 0.2 % due to the increased uncertainty of the thermophysical properties of the mixture relative to those of pure R125 that are required for the work correction ( $W_{PV}$ ). The expanded uncertainties of the original measurements and the resulting combined uncertainties are shown in Table 1.

### Heat Capacity and Density Results

As mentioned in the discussion of eq 2, adjustments are applied to the raw heat capacity data to account for the

**Table 1. Expanded Uncertainties (Coverage Factor  $k = 2$ ) of the Measurements with the Adiabatic Differential Calorimeter**

absolute temperature	0.03 K
temperature difference	0.7 mK
pressure (R410A)	2 kPa
mass	2 mg
volume	0.07 cm <sup>3</sup>
mixture mass fraction	0.0002
density	0.2 %
electrical energy	0.02 %
power difference, $\Delta Q$	1 J·K <sup>-1</sup>
change-of-volume work	0.5 %
heat capacity at constant volume	2 % for liquid, increasing to 4 % for gas below its critical density

change-of-volume work of the bomb. During a measurement sequence, the volume of the bomb varies with temperature and pressure in accordance with formulas reported previously.<sup>3</sup> The term  $W_{PV}$  is an important adjustment since the bomb is thin-walled. Referring to Goodwin and Weber,<sup>4</sup> we can obtain the work from

$$W_{PV} = \left( T_2 \left( \frac{\partial P}{\partial T} \right)_{V_2} - \frac{1}{2} \Delta P \right) \Delta V \quad (3)$$

where  $\Delta P = P_2 - P_1$  is the pressure rise and  $\Delta V = V_2 - V_1$  is the change of volume. The pressure derivative is obtained from an equation of state. Accurate values for the pressure derivative were required, since this quantity has a significant influence on the adjustment for the change of volume work. Estimates of this derivative were calculated with values for the Helmholtz energy from the NIST REFPROP 7.0<sup>5</sup> database, which uses the equations of state of Lemmon and Jacobsen.<sup>6,7</sup>

A minor adjustment was applied to the mass enclosed in the bomb. The total mass of the sample was corrected by deducting the mass residing in the noxious volume, which consists of the combined volumes of the connecting tubing, the charging valve body, and the pressure transducer. In total, the noxious volume was approximately 0.4 % of the bomb volume. This amount was calculated from densities from an equation of state<sup>6,7</sup> and the noxious volume obtained from previous calibrations.<sup>3</sup>

**Pure R125.** The heat capacity data  $C_V$  of each run are presented in the Supporting Information for this paper at a total of 641 single-phase liquid and gaseous states. The final temperature ( $T$ , ITS-90) of the heating interval is provided without the corresponding pressure. The pressure transducer exhibited unusual drift in its vacuum reading that was on the order of 0.02 MPa during the R125 measurements. This increased pressure uncertainty did not significantly impact the measured density and heat capacity data, but made it inadvisable to use the measurements as a source of  $P\rho T$  data, so pressure is not reported for R125. The densities  $\rho$  of 641 states were calculated from the measured sample mass and the calibrated bomb volume at each measured temperature and pressure.

Figure 1 shows the range of the measured temperatures and pressures along nine isochores and their relationship to the calculated vapor pressure boundary for R125. The measured pressures range up to 20 MPa at temperature increments of 1 K. The nine isochores cover a range of densities from 0.4 g·cm<sup>-3</sup> to 1.2 g·cm<sup>-3</sup>. Figure 2 shows the measured isochoric specific heat capacities at constant volume for R125. The specific heat increases significantly near the gas–liquid critical point of R125 ( $T_c = 339.17$  K,  $P_c = 3.6177$  MPa,  $\rho_c = 0.57358$  g·cm<sup>-3</sup>).<sup>6</sup> Relative deviations between the experimental heat capacities and values calculated with the Helmholtz free energy formulation of

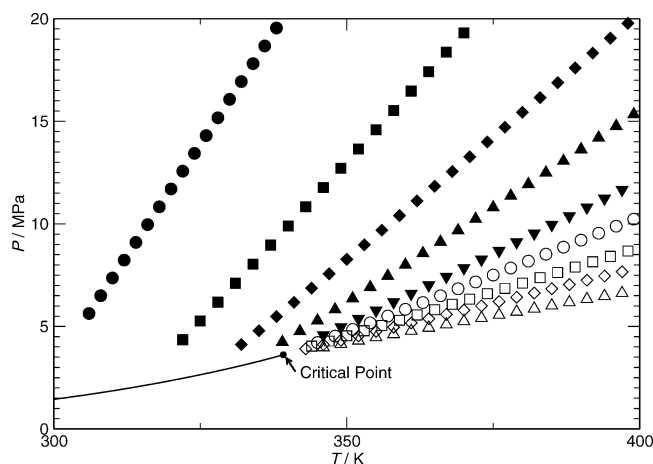


**Figure 1.** Measured pressure and temperature states along isochores relative to the vapor–liquid saturation boundary<sup>5,6</sup> (solid line) for R125. The reduced density ( $\rho/\rho_c$ ) of each isochore is designated by the symbols:  $\triangle$ , 0.70;  $\diamond$ , 0.88;  $\square$ , 1.02;  $\circ$ , 1.20;  $\nabla$ , 1.35;  $\blacktriangle$ , 1.54;  $\blacklozenge$ , 1.70;  $\blacksquare$ , 1.88;  $\bullet$ , 2.09.

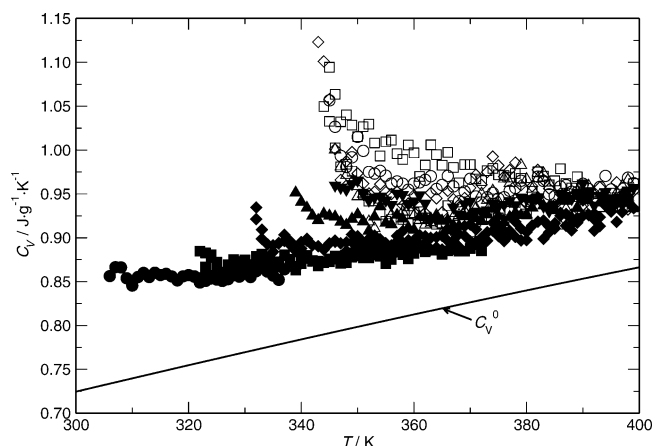


**Figure 2.** Measured specific heat at constant volume along isochores for R125. Calculated ideal gas specific heat<sup>5,6</sup> is also shown. The reduced density ( $\rho/\rho_c$ ) of each isochore is designated by the symbols:  $\triangle$ , 0.70;  $\diamond$ , 0.88;  $\square$ , 1.02;  $\circ$ , 1.20;  $\nabla$ , 1.35;  $\blacktriangle$ , 1.54;  $\blacklozenge$ , 1.70;  $\blacksquare$ , 1.88;  $\bullet$ , 2.09.

Lemmon and Jacobsen<sup>6</sup> are shown in Figure 3. The deviations are calculated relative to values from the equation of state and the experimental temperature and density. Deviations from the model of Lemmon and Jacobsen<sup>6</sup> are generally less than 5 %, with the largest deviations observed for the low-density gas near or below the critical density. This is the region where the experimental data have their highest uncertainty of 4 %. The higher density liquid specific heat values generally agree with the model to within 2 %. The experimental specific heat values deviate up to 7 % from the calculated values for gas isochores near the critical density over the temperature range from 340 K to 355 K. The maximum deviations shown in Figure 3 are slightly larger than expected based on the combined uncertainty of the lowest density isochors of  $\pm 4$  % and the estimated uncertainty of  $\pm 0.5$  % for specific heat from the equation of state.<sup>6</sup> However, it should be kept in mind that the equation of state<sup>6</sup> was optimized for all available property data, including density, sound speed, isochoric, and isobaric specific heat.

Figure 4 shows the relative deviations between the present specific heat measurements and the earlier measurements of Lüddecke and Magee<sup>1</sup> in the high-density

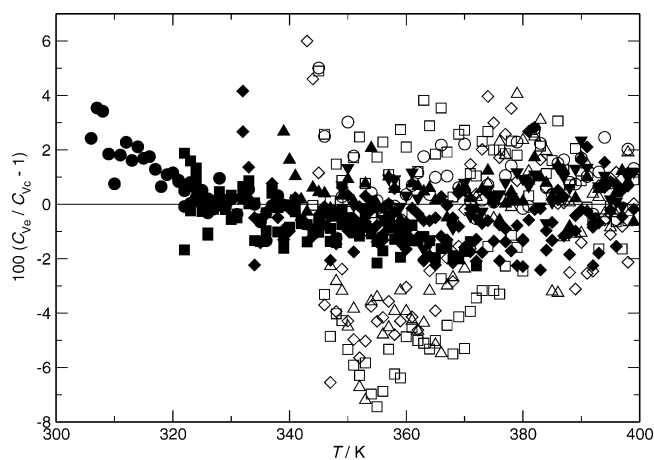


**Figure 3.** Relative deviations between the measured specific heats at constant volume ( $C_{V_e}$ ) and the values calculated with REFPROP 7.0<sup>5,6</sup> ( $C_{V_c}$ ) for R125. The reduced density ( $\rho/\rho_c$ ) of each isochore is designated by the symbols:  $\triangle$ , 0.70;  $\diamond$ , 0.88;  $\square$ , 1.02;  $\circ$ , 1.20;  $\nabla$ , 1.35;  $\blacktriangle$ , 1.54;  $\blacklozenge$ , 1.70;  $\blacksquare$ , 1.88;  $\bullet$ , 2.09.

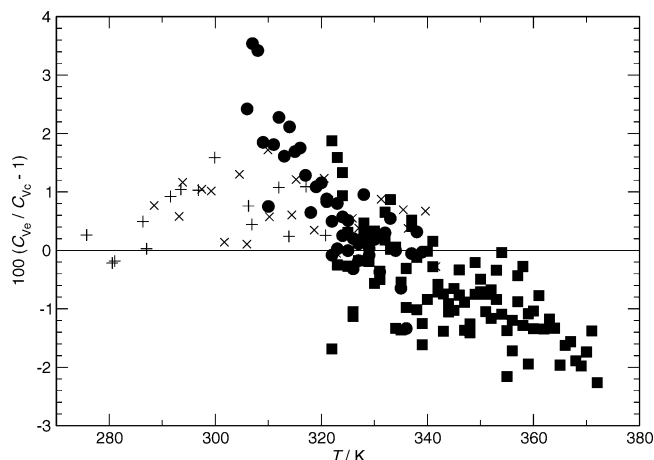


**Figure 4.** Relative deviations between the measured specific heats at constant volume ( $C_{V_e}$ ) and the values calculated with REFPROP 7.0<sup>5,6</sup> ( $C_{V_c}$ ) for R125. The two lowest density isochores of Lüddecke and Magee<sup>1</sup> are shown with  $\times$  ( $\rho/\rho_c = 2.20$ ) and  $+$  ( $\rho/\rho_c = 2.32$ ) symbols, while the two highest density isochores reported in this work are shown with  $\blacksquare$  ( $\rho/\rho_c = 1.88$ ) and  $\bullet$  ( $\rho/\rho_c = 2.09$ ) symbols.

liquid region where the densities are comparable. The model of Lemmon and Jacobsen<sup>6</sup> provides the baseline for this comparison. There is good agreement between the earlier measurements made with an adiabatic calorimeter operated in a heat pulse mode and the present measurements made with a twin-bomb adiabatic calorimeter operated in a scanning mode. The present measurements have a larger uncertainty than the measurements of Lüddecke and Magee.<sup>1</sup>

**R410A Mixture.** The heat capacity data  $C_V$  of each run are presented in the Supporting Information for this paper at a total of 402 single-phase liquid and gaseous states. The final temperature ( $T$ , ITS-90) and pressure ( $p$ ) of the heating interval are presented. The densities ( $\rho$ ) of 402 states were calculated from the measured sample mass and the calibrated bomb volume at the measured temperatures and pressures. All measurements were made on the same gravimetrically prepared mixture sample. This sample was well-mixed and remained heated and single phase while the vapor was condensed into the cold apparatus. The apparatus was sealed with single-phase liquid at the

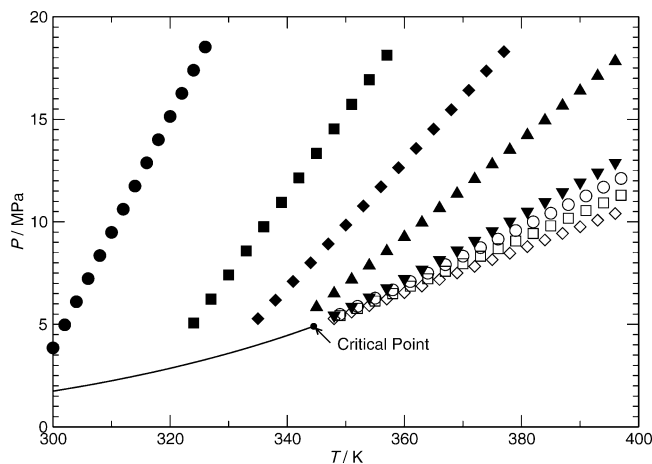


**Figure 5.** Measured pressure and temperature states along isochores relative to the bubble-point locus,<sup>5,7</sup> which is nearly equivalent to the dew-point locus for the R410A mixture. The reduced density ( $\rho/\rho_c$ ) of each isochore is designated by the symbols:  $\diamond$ , 1.03;  $\square$ , 1.14;  $\circ$ , 1.24;  $\nabla$ , 1.34;  $\blacktriangle$ , 1.65;  $\blacklozenge$ , 1.87;  $\blacksquare$ , 2.06;  $\bullet$ , 2.33.

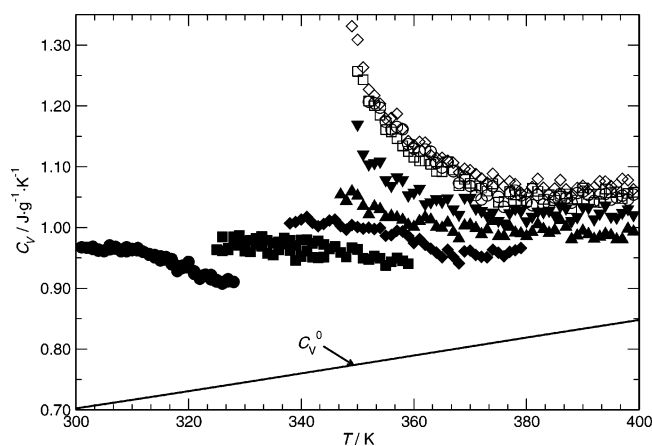


**Figure 6.** Measured specific heats at constant volume along isochores for the R410A mixture. Calculated ideal gas specific heat<sup>5,7</sup> is also shown. The reduced density ( $\rho/\rho_c$ ) of each isochore is designated by the symbols:  $\diamond$ , 1.03;  $\square$ , 1.14;  $\circ$ , 1.24;  $\nabla$ , 1.34;  $\blacktriangle$ , 1.65;  $\blacklozenge$ , 1.87;  $\blacksquare$ , 2.06;  $\bullet$ , 2.33.

desired density for a given isochore. Thus, the composition of the sample remained constant and well-known throughout the measurements.

Figure 5 shows the range of the measured temperatures and pressures along eight isochores and their relationship to the calculated bubble-point locus. The measured pressures range up to 20 MPa at temperature increments of 1 K. The eight isochores cover a range of densities from  $0.47 \text{ g}\cdot\text{cm}^{-3}$  to  $1.07 \text{ g}\cdot\text{cm}^{-3}$ . Figure 6 shows the measured specific heat capacities for R410A. As for pure R125, the specific heat increases significantly near the gas–liquid critical point calculated for R410A with the model of Lemmon and Jacobsen<sup>7</sup> ( $T_c = 344.51 \text{ K}$ ,  $P_c = 4.9026 \text{ MPa}$ ,  $\rho_c = 0.45953 \text{ g}\cdot\text{cm}^{-3}$ ). Relative deviations between the experimental heat capacities and densities and the values calculated with the Helmholtz free energy formulation of Lemmon and Jacobsen<sup>7</sup> are shown in Figures 7 and 8, respectively. The mixture model calculations agree with the experimental specific heat data to within  $\pm 4 \%$ . The uncertainty for specific heats calculated with the mixture model<sup>7</sup> is  $\pm 0.5 \%$ . Thus, good agreement, which is comparable to the uncertainty of the specific heat data, is found between the mixture model and the present data. The mixture model

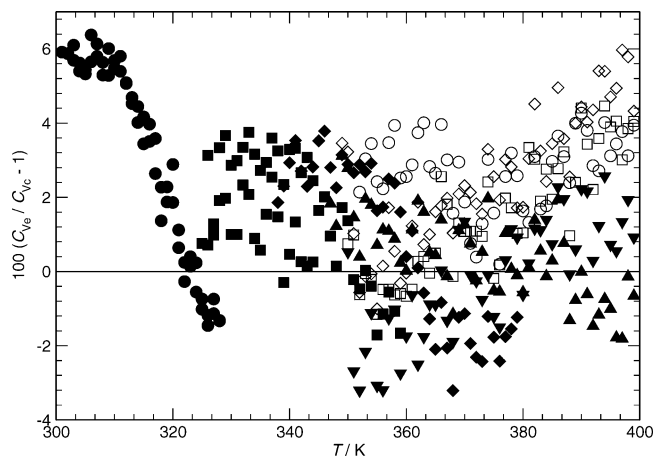


**Figure 7.** Relative deviations between the measured specific heats at constant volume ( $C_{V,e}$ ) and the values calculated with REFPROP 7.0<sup>5,7</sup> ( $C_{V,c}$ ) for the R410A mixture. The reduced density ( $\rho/\rho_c$ ) of each isochore is designated by the symbols:  $\diamond$ , 1.03;  $\square$ , 1.14;  $\circ$ , 1.24;  $\nabla$ , 1.34;  $\blacktriangle$ , 1.65;  $\blacklozenge$ , 1.87;  $\blacksquare$ , 2.06;  $\bullet$ , 2.33.

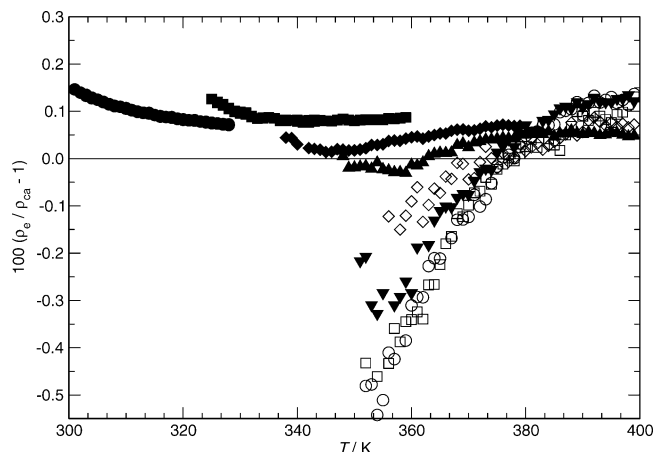


**Figure 8.** Relative deviations between the measured densities ( $\rho_e$ ) and the values calculated with REFPROP 7.0<sup>5,7</sup> ( $\rho_{c,a}$ ) for the R410A mixture. The reduced density ( $\rho/\rho_c$ ) of each isochore is designated by the symbols:  $\diamond$ , 1.03;  $\square$ , 1.14;  $\circ$ , 1.24;  $\nabla$ , 1.34;  $\blacktriangle$ , 1.65;  $\blacklozenge$ , 1.87;  $\blacksquare$ , 2.06;  $\bullet$ , 2.33.

calculations generally agree with the experimental densities to within 0.2 %, except near the mixture critical point, where the experimental densities are systematically lower than the calculated densities by up to 0.5 %.

## Conclusions

The isochoric heat capacity ( $C_V$ ) was measured as a function of temperature and density for a total of 641 single-phase states of R125. The isochoric heat capacity ( $C_V$ ) and density were measured as a function of temperature and pressure for a total of 402 single-phase states of a gravimetrically prepared mixture of R410A. These measurements agree well with previous heat capacity measurements and the Helmholtz free energy models of Lemmon and Jacobsen<sup>6,7</sup> for the specific heat of both R125 and R410A and for the density of R410A.

## Supporting Information Available:

Tabulated experimental data for the specific heat at constant volume of R125 and R410A. This material is available free of charge via the Internet at <http://pubs.acs.org>.

## Literature Cited

- (1) Lüdecke, T. O.; Magee, J. W. Molar heat capacity at constant volume of difluoromethane (R32) and pentafluoroethane (R125)

- from the triple-point temperature to 345 K at pressures to 35 MPa. *Int. J. Thermophys.* **1996**, *17*, 823–849.
- (2) Magee, J. W. Isochoric heat capacity measurements for binary refrigerant mixtures containing difluoromethane (R32), pentafluoroethane (R125), 1,1,1,2-tetrafluoroethane (R134a), and trifluoroethane (R143a) from 200 to 345 K at pressures to 35 MPa. *Int. J. Thermophys.* **2000**, *21*, 95–111.
- (3) Magee, J. W.; Blanco, J. C.; Deal, R. J. High-temperature adiabatic calorimeter for constant-volume heat capacity of compressed gases and liquids. *J. Res. Natl. Inst. Stand. Technol.* **1998**, *103*, 63–75.
- (4) Goodwin, R. D.; Weber, L. A. Specific heats  $C_v$  of fluid oxygen from the triple point to 300 K at pressures to 350 atmospheres. *J. Res. Natl. Bur. Stand.* **1969**, *73A*, 15–24.
- (5) Lemmon, E. W.; McLinden, M. O.; Huber, M. L. *REFPROP*, Reference Fluid Thermodynamic and Transport Properties (NIST Standard Reference Database 23), Version 7.0; National Institute of Standards and Technology: Gaithersburg, MD, 2002.
- (6) Lemmon, E. W.; Jacobsen, R. T. A new functional form and new fitting techniques for equations of state with application to pentafluoroethane (HFC-125). *J. Phys. Chem. Ref. Data* **2005**, *34*, 69–108.
- (7) Lemmon, E. W.; Jacobsen, R. T. Equations of state for mixtures of R-32, R-125, R-134a, R143a, and R152a. *J. Phys. Chem. Ref. Data* **2004**, *33*, 593–620.

Received for review May 12, 2005. Accepted July 1, 2005. We thank the Building Technologies Program of the U.S. Department of Energy for partial support of these measurements.

JE0501843